Plane Wave Based Near-Field Far-Field Transformation with Adaptive Field Translations

Carsten H. Schmidt, ***M. Ayyaz Qureshi***, and ***Thomas F. Eibert***
Lehrstuhl für Hochfrequenztechnik, Technische Universität München,
Arcisstr. 21, 80333 Munich, Germany,
carstenschmidt@tum.de

Abstract

Near-field transformation algorithms compute the antenna radiation pattern from a measurement in the radiating near field. The plane wave based near-field transformation algorithm has a low numerical complexity while achieving full probe correction and it is furthermore applicable to arbitrary measurement grids giving a huge flexibility for near-field probing. The transmission equation for a set of measurement points is evaluated in a multilevel fashion and the field translations are now carried out on different levels depending on the distance of the measurement point from the antenna. The adaptive field translations allow to enhance the accuracy of the transformed far-field pattern.

1 Introduction

The radiation pattern of an antenna under test (AUT) is commonly measured by far-field, compact range, or near-field techniques [1]. Far-field measurements suffer from the huge space that is required to measure electrically large antennas and also from environmental effects if measured outdoors. Compact range measurements can be carried out indoors in controlled measurement facilities but especially the large reflectors for measurements at lower frequencies are rather expensive. Near-field measurements are conducted in anechoic chambers and the field distribution is measured in the radiating near-field. Therefore a post-processing near-field far-field transformation is required to compute the far-field pattern [2]. Near-field transformation algorithms model the radiation behavior of the AUT by a set of equivalent sources. These equivalent sources are set into relation to the measured probe signals by a transmission formula and are obtained as solution of the inverse field problem. For measurements in the near field the influence of the field probe has to be considered since it is rather integrating the field strength around the measurement point than measuring at a discrete point due to its finite extension. This has to be considered when setting up the transmission formula and is called probe correction.

Classical algorithms for near-field far-field transformation use eigenmode expansions of the underlying coordinate system of the measurement system such as spherical multipoles for spherical near-field measurements [3] and plane waves in a halfspace for planar near-field measurements [4]. These techniques evaluate orthogonality properties of the eigenmodes and thus require measurements on regularly sampled grids.

In this paper the multilevel plane wave based near-field far-field transformation with low numerical complexity, full probe correction capabilities, and the ability to handle arbitrary measurement grids is revisited. The focus is to enhance the flexibility of the field translations so that they can be utilized on various levels. This allows to optimize the accuracy of the transformed far-field patterns and the runtime.

2 Plane Wave Based Near-Field Far-Field Transformation

The plane wave based near-field transformation [5,6] utilizes plane waves $\tilde{\boldsymbol{J}}(\hat{k})$, which are assumed for all spatial directions, as equivalent sources. The probe signal is computed by translating the plane waves to the measurement point $\boldsymbol{r}_{\mathrm{M}}$ utilizing the diagonal translation operator $T_L(\hat{k}, \hat{r}_{\mathrm{M}})$, known from fast multipole methods (FMM) [7]. The planes waves are then weighted with the probe far-field pattern $\bar{\boldsymbol{P}}(\hat{k}, \boldsymbol{r}_{\mathrm{M}})$ and

978-1-4244-6051-9/11/$26.00

superimposed coherently. In order to achieve a low numerical complexity of $O(N \log N)$ the measurement points are grouped in a hierarchical multilevel box structure, as seen in Fig. 1.

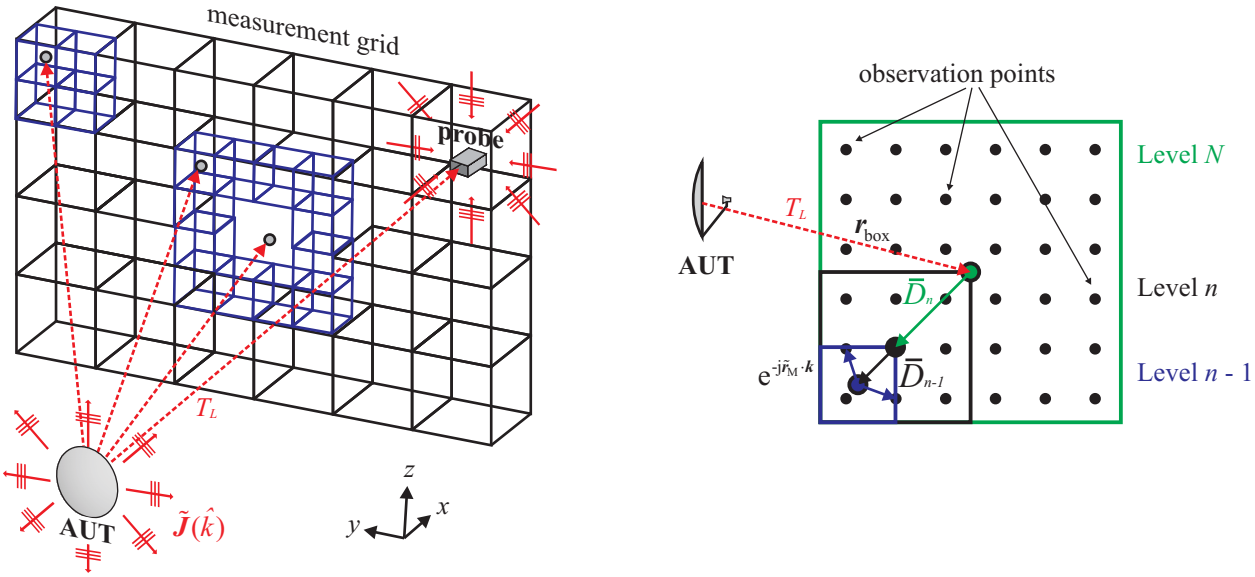

Figure 1: Setup for multilevel plane wave based processing of near-field measurement. Left: hierarchical measurement point grouping. The subdivision into smaller boxes is just shown for the box on the upper left corner for simplicity. Right: disaggregation.

The field translations

$$\tilde{\boldsymbol{J}}_N^{i_N}(\hat{k}) = T_L(\hat{k}, \hat{r}_{\text{box}}) \left(\bar{\boldsymbol{I}} - \hat{k}\hat{k}\right) \cdot \tilde{\boldsymbol{J}}(\hat{k}) \tag{1}$$

are then carried out to the box centers on the highest level i_N only instead to all measurement points explicitly. The plane wave spectra

$$\tilde{\boldsymbol{J}}_n^{i_n}(\hat{k}) = \bar{\boldsymbol{D}}_n^{i_n}(\boldsymbol{k}, \boldsymbol{r}_n^{i_n}) \cdot \left(\bar{\boldsymbol{I}} - \hat{k}\hat{k}\right) \cdot \tilde{\boldsymbol{J}}_{n+1}^{i_{n+1}}(\hat{k}) \tag{2}$$

are further processed through the levels by disaggregation and anterpolation where

$$\bar{\boldsymbol{D}}_n^{i_n}(\boldsymbol{k}, \boldsymbol{r}_n^{i_n}) = \bar{\boldsymbol{V}}_n(\hat{k}) \mathrm{e}^{-\mathrm{j}\boldsymbol{r}_n^{i_n} \cdot \boldsymbol{k}} \tag{3}$$

is the disaggregation and anterpolation operator. Disaggregation is a simple phase shift between the box centers on level i_{n+1} and level i_n or finally the box center on the lowest level and the measurement point (see Fig. 1 right). Anterpolation can be seen as adjoint operation to interpolation and reduces the sampling rate of the plane wave spectra with decreasing box size. This is possible since the spectral content of the plane wave spectra is proportional to the box size. The probe signal

$$U(\boldsymbol{r}_{\text{M}}) = -\mathrm{j}\frac{\omega\mu_0}{4\pi} \sum_{k_\varphi} \sum_{k_\vartheta} W_\vartheta^{k_\vartheta, L} W_\varphi^L \mathrm{e}^{-\mathrm{j}\tilde{\boldsymbol{r}}_{\text{M}} \cdot \boldsymbol{k}} \bar{\boldsymbol{P}}(\hat{k}, \boldsymbol{r}_{\text{M}}) \cdot \left(\bar{\boldsymbol{I}} - \hat{k}\hat{k}\right) \cdot \tilde{\boldsymbol{J}}_0^{i_0}(k_\varphi, k_\vartheta) \tag{4}$$

is obtained by applying the final phase shift to the measurement points and weighting the plane waves with the probe's far-field pattern. The integral is evaluated by numerical quadrature with the quadrature weights $W_\vartheta^{k_\vartheta, L}$ and W_φ^L.

The algorithm is implemented within an iterative generalized minimum residual (GMRES) solver [8] in an on-the-fly manner.

3 Adaptive Field Translations

In order for the plane wave representation to converge, the AUT and measurement point boxes must not overlap. This requirement is not very strict but in order to obtain a good accuracy of the transformed far-field pattern a larger separation between AUT and receiving boxes is recommended. This is implemented by introducing buffer boxes. The transformation is now extended such that field translations can be carried out to boxes on different levels depending on their distance from the AUT. Thus it is possible to have larger boxes further away from the antenna while maintaining the required number of buffer boxes for the whole setup. In this way only boxes close to the AUT have to use lower levels for translations and thus less levels in total. With adaptive field translations one is able to find a good compromise between large boxes in the whole setup giving small computation time and less accuracy versus small boxes in the whole setup giving larger computation time and higher accuracy.

An example for a planar measurement setup is shown in Fig. 1 left. The black boxes near the edges of the measurement plane have a relatively large distance from the AUT whereas the blue boxes closer to the center have a smaller distance from the AUT. The box sizes and numbers of levels are chosen accordingly. The subdivision into smaller boxes is just shown for the box on the upper left corner for simplicity. If required, field translations to measurement points very close to the AUT can also be considered directly, as for the points in the center of the measurement plane shown in Fig. 1 left.

4 Results

For validation of the adaptive field translations, a planar measurement setup is considered due to the large variation in the measurement distance. The AUT is a horn antenna synthesized by a distribution of electric dipoles at 3 GHz and the probe antenna consists of four electric dipoles. The generation of the synthetic data follows the description in [9]. The measurement plane has a size of 4 m x 4 m and is sampled equidistantly with a step size of $\lambda/2$. Transformations are carried out for two different configurations as described in Table 1. Columns 2 - 6 show the number of measurement points which are handled on each translation level, e.g. in column 4 the transformation for these points is carried out using a recursive box structure with three levels. Column 7 shows the relative near-field error which gives the deviation of the probe signals computed from the solution of the algorithm with respect to the measured probe signals. The residuum of the iterative solver was set to 1e-4, the accuracy can be further enhanced by lowering the residuum.

Table 1: Configurations for multilevel plane wave based processing of near-field measurement.

Configuration	points L1	points L2	points L3	points L4	points L5	near-field error
I	0	0	0	0	6 561	1.84e-2
II	1 101	640	1 492	2 916	412	1.23e-3

The transformed far-field patterns for both configurations are shown in Fig. 2 in an E- and H-plane cut together with their respective error levels and the reference solution. The region of valid angle is shown in white. An enhanced accuracy is evident for the measurement utilizing adaptive field translations.

5 Conclusion

The plane wave based near-field far-field transformation algorithm with low numerical complexity, full probe correction capabilities, and the applicability for arbitrary measurement grids has been presented. In this contribution adaptive field translations have been utilized to handle variable distances between AUT

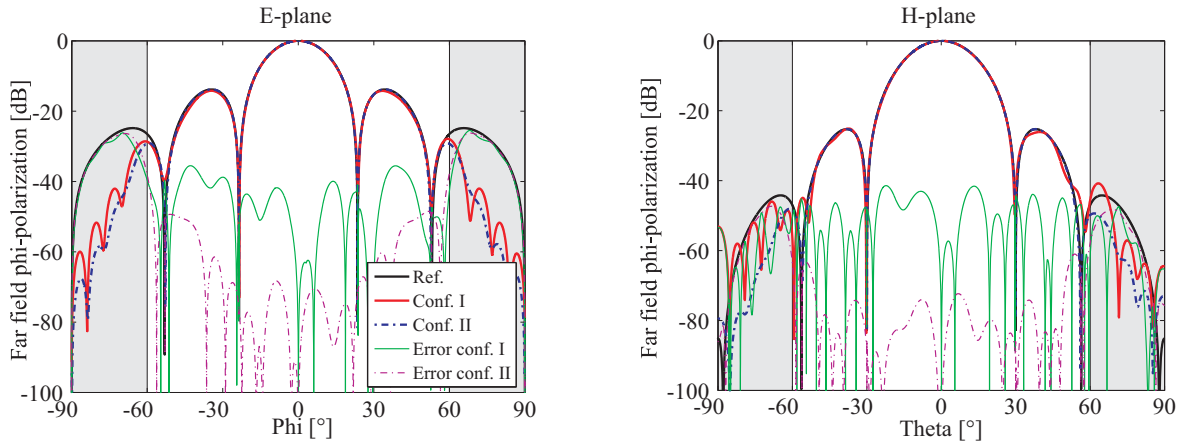

(a) E-plane cut.

(b) H-plane cut.

Figure 2: Comparison of transformed far-field patterns for configurations I and II according to Table 1.

and the measurement points with hierarchical box structures of different numbers of levels. In this way the accuracy of the transformed far-field pattern can be optimized as a compromise between large translation boxes resulting in less buffer boxes, small runtime, and less accuracy and small translation boxes resulting in more buffer boxes, larger runtime, and higher accuracy.

6 References

1. C. A. Balanis, *Modern Antenna Handbook*, John Wiley & Sons, Inc., 2008.

2. A. D. Yaghjian, "An Overview of Near-Field Antenna Measurements," *IEEE Trans. Antennas Propag.*, vol. 34, no.1, January 1986, pp. 30–45.

3. J. E. Hansen, *Spherical Near-Field Antenna Measurements*, Peter Peregrinus, London, 1988.

4. D. Kerns, "Plane-Wave Scattering-Matrix Theory of Antennas and Antenna-Antenna Interactions," *National Bureau of Standards*, Boulder CO, 1981.

5. C. H. Schmidt, M. M. Leibfritz, and T. F. Eibert, "Fully Probe-Corrected Near-Field Far-Field Transformation Employing Plane Wave Expansion and Diagonal Translation Operators," *IEEE Trans. Antennas Propag.*, vol. 56, no. 3, March 2008, pp. 737–746.

6. C. H. Schmidt and T. F. Eibert, "Multilevel Plane Wave Based Near-Field Far-Field Transformation for Electrically Large Antennas in Free-Space or Above Material Halfspace,"' *IEEE Trans. Antennas Propag.*, vol. 57, no. 5, May 2009, pp. 1382–1390.

7. W. Chew, J. Jin, E. Michielssen, and J. Song, *Fast and Efficient Algorithms in Computational Electromagnetics*, Artech House, Inc. 2001.

8. Y. Saad, *Iterative Methods for Sparse Linear Systems*, 2nd ed., Society for Industrial and Applied Mathematics, 2003.

9. C. H. Schmidt, D. T. Schobert, and T. F. Eibert, "Electric Dipole Based Data Generation for Probe-Corrected Near-Field Antenna Measurements," 5th European Conference on Antennas and Propagation, Rome, Italy, April 2011.